Supporting Information for

Insulin Fibril Inhibition Using Glycopolymeric Nanoassemblies

Avisek Bera,[a,#] Pooja Ghosh,[a,#] Soumen Barman,[b] Sagnik Bhattacharya,[a,c] Babu Sudhamalla,[b] Kalyan Goswami,[d] and Priyadarsi De[a,*]

[a]Polymer Research Centre and Centre for Advanced Functional Materials, Department of Chemical Sciences, Indian Institute of Science Education and Research Kolkata, Mohanpur - 741246, Nadia, West Bengal, India.

[b]Department of Biological Science, Indian Institute of Science Education and Research Kolkata, Mohanpur - 741246, Nadia, West Bengal, India.

[c]School of Chemical Sciences, National Institute of Science Education and Research Bhubaneswar, Jatni - 752050, Khurda, Odisha, India.

[d]Department of Biochemistry, All India Institute of Medical Sciences (AIIMS), Kalyani, Basantapur, NH-34 connector, Kalyani - 741245, Nadia, West Bengal, India.

*Corresponding Author: p_de@iiserkol.ac.in

[#]These authors contributed equally in this manuscript

Experimental Details

Materials. *Tert*-butoxycarbonyl (Boc)-L-leucine (Boc-L-Leu-OH, 99%), dicyclohexylcarbodiimide (DCC, 99%), 4-dimethylaminopyridine (DMAP, 99%), *β*-D-glucose pentaacetate (98%), borontrifluoride diethyl etherate (BF_3•Et_2O, 46.5%), 2-hydroxyethyl methacrylate (HEMA, 97%), thioflavin T (ThT), nile red (NR), pyrene (98%), anhydrous *N,N*-dimethylformamide (DMF, 99.9%), and Dowex 50WX8 were purchased from Sigma and used directly without any further purification. Insulin ex. bovine pancreas (97%) and trifluoroacetic acid (TFA, 99.5%) were purchased from Sisco Research Laboratories Pvt.

Ltd. (SRL), India. The 2,2′-azobis(isobutyronitrile) (AIBN, 98%) was bought from Sigma and recrystallized from methanol. NMR solvents like DMSO-d_6 (99.9% D), $CDCl_3$ (99.8% D), and D_2O (99% D) were procured from Cambridge Isotope Laboratories, Inc., USA. Solvents, including ethyl acetate, acetone, tetrahydrofuran (THF), dichloromethane, and hexanes (a combination of isomers) were used after simple distillation-based purification. All the experiments were conducted using Milli-Q grade water. 4-Cyano-4-(dodecylsulfanylthiocarbonyl)sulfanylpentanoic acid (CDP) was prepared following a literature report.[1]

Instrumentation. The number average molecular weights ($M_{n,SEC}$) and molecular weight distributions (dispersity, $Đ$) of the polymers were determined in a size exclusion chromatography (SEC) instrument in tetrahydrofuran (THF) at 30 °C using a flow rate of 0.8 mL/min. The SEC instrument is connected to a Waters 1515 HPLC pump, a Waters 2414 refractive index (RI) detector, one PolarGel-M guard column (50 × 7.5 mm), and two PolarGel-M analytical columns (300 × 7.5 mm). To calibrate the instrument, poly(methyl methacrylate) (PMMA) standards with narrow $Đ$ values were used. The ^{1}H NMR spectroscopy was carried out in a 5 mm diameter tube in deuterated solvents on a Bruker AvanceIII 500 MHz spectrometer or 400 MHz JEOL ECS NMR spectrometer at 25 °C. The absorbance study and fluorescence assays were performed using Perkin Elmer Lambda 35 UV-visible spectrophotometer and Horiba JobinYvon (Fluoromax-3, Xe-150 W, 250-900 nm) fluorescence spectrophotometer, respectively. A JEOL JEM-2100F electron microscope operating at 120 kV voltage was used to capture transmission electron microscopy (TEM) pictures. A Jasco J-815 circular dichroism (CD) spectrometer was used for CD spectroscopic examination. Using a Zetasizer Nano ZS instrument (Malvern Instruments Ltd, UK), dynamic light scattering (DLS) measurements were performed. The DLS instrument is equipped with a He-Ne laser, operating at 633 nm. The scattering angle was fixed at 173°. A confocal laser

scanning microscope (Axio Observer A1) from Zeiss was used to perform fluorescence lifetime imaging microscopy (FLIM) measurements, and 40X objectives were used together with a DCS-120 system from Becker & Hickl (BH) GmbH. Isothermal titration calorimetry (ITC) experiments were carried out with a MICROCAL PEAQ-ITC (Malvern) instrument.

Synthesis of Boc-Leu-HEMA monomer. For the synthesis of Boc-Leu-HEMA (**1**, see Scheme S1), we followed previous literature.[2] The Boc-L-Leu-OH (10.0 g, 43.2 mmol) was dissolved in dry dichloromethane (DCM, 100 mL), and kept in a 250 mL round bottom flask in an ice-water bath under stirring condition. Dicyclohexylcarbodiimide (DCC, 10.7 g, 51.9 mmol) and 4-dimethylaminopyridine (DMAP, 1.0 g, 8.6 mmol) in 15 mL of dry DCM was then added dropwise to the above solution. Next, 2-hydroxyethyl methacrylate (HEMA, 6.8 g, 51.9 mmol) was added in a dropwise manner, and after 30 min the ice-water bath was removed. The mixture was stirred at room temperature for a period of 24 h. Next, the solution was filtered to remove *N,N′*-dicyclohexylurea (DCU). The filtrate was washed with 1.0 N HCl, $NaHCO_3$ solution, brine solution, and dried over anhydrous sodium sulfate (Na_2SO_4). Finally, the pure Boc-Leu-HEMA monomer was obtained (yield: 81%) by purifying it using silica gel column chromatography employing hexanes/ethyl acetate (3:1, v/v) as the mobile phase.

Synthetic procedure of side chain carbohydrate containing monomer. For the synthesis of Ac-G-EMA (**2**, see Scheme S2), we followed previous literature.[3] Typically, *β*-D-glucose pentaacetate (8.3 g, 21.2 mmol) and borontrifluoride diethyl etherate (BF_3•Et_2O, 8.2 g, 57.7 mmol) in anhydrous dichloromethane (80 mL), 6.0 g of molecular sieves (4 Å) was added in stirred condition. Then, the mixture was allowed to cool at 5 °C under nitrogen atmosphere, and HEMA (5.0 g, 38.4 mmol) was added into the mixture in a dropwise manner. The solution was further stirred for a period of 48 h at 25 °C. Next, the suspension solution was filtered and washed with brine solution and dried over anhydrous Na_2SO_4. To get the pure monomer Ac-G-EMA (**2**), the crude product was then purified by silica gel column chromatography

employing a hexanes/ethyl acetate solvent mixture (4:1, v/v) as the mobile phase. The final product was obtained as a white coloured solid compound (yield: 77%).

Self-assembly process and critical aggregation concentrations (CAC) determination. Since our synthesized polymers contain both hydrophobic and hydrophilic segments, therefore they readily undergo self-assembly in aqueous medium. To confirm the self-assembly process, we have determined the CAC values of the polymers. The CAC values of different glycosylated amino acid-based block copolymers were calculated using a spectrofluorometer using pyrene as a fluorescent hydrophobic probe.[4] A fixed amount of pyrene in acetone was prepared and added to different concentrations of aqueous polymer solutions in glass vials, and the final concentration of pyrene was maintained at 10^{-7} mol/L in each sample solution. Then, the glass vials were left open overnight at room temperature for complete evaporation of acetone. The fluorescence emission intensities of the samples were recorded upon exciting the samples at 337 nm, and the spectra were scanned in the region of 360-480 nm, keeping the fixed slit width at 5 nm for both excitation and emission. The ratios of fluorescence emission intensity, I_{393}/I_{373}, were plotted against the logarithm of the concentrations of the copolymers, and the CAC values were determined from the intersecting point of the two tangent plots.

Insulin fibril formation in the presence of glycopolymers. For the synthesis of *in vitro* insulin fibril, we followed previous literature report where fibril was obtained after incubation of native insulin (1 mg/mL) directly in HCl solution (10 mM; pH 2) at 65 °C for 24 h under constant stirring at 250 rpm.[5] To find the effect of glycopolymers on the fibrillation process, we added 2 mg of different glycopolymers into the native insulin solution (1 mg/mL) keeping other conditions same, and the samples were kept under incubation for 24 h.

Thioflavin T (ThT) fluorescence assay. For *in vitro* quantification and identification of insulin fibrils formation, a ThT fluorescence assay was performed.[6] Typically, aliquots were

taken from the respective sets of samples, and 1 mM of ThT stock solution in methanol was added into the Tris-HCl buffer (50 mM; pH 8), keeping the final concentration of samples at 2 μM and ThT at 5 μM.[7] Then, the solutions were allowed to incubate for 20 min, and the fluorescence of the solution was measured at 482 nm upon excitation at 450 nm, keeping the slit width fixed at 5 nm (integration time = 0.3 sec) for both excitation and emission measurements. For ThT kinetic experiments, sample aliquots were taken at different time from 0 to 24 h for each set of samples. Then, incubation of the samples with stock solution of ThT was performed for a period of 20 min, and fluorescence spectra were taken.

Nile red (NR) fluorescence assay. To perform the NR fluorescence assay, at first, 1 mM NR solution in methanol was prepared. This dye solution was then mixed with different samples and the volume was adjusted with Tris-HCl buffer (50 mM; pH 8) to maintain the final concentration of samples at 2.5 μM and dye at 10 μM.[8] After 20 min incubation, the fluorescence emission spectra were measured in the region of 540-800 nm upon exciting at 530 nm wavelength. During the experiment, 0.3 s integration time and slit width = 5 nm were used.

Turbidity assay. To confirm the extent of fibril formation alone and in the presence of different glycopolymeric aggregates, a turbidity assay was performed using a UV-Vis spectrophotometer, where we measured the absorbances of different samples at 350 nm.[9] For this measurement, 5 μM concentration of each sample was prepared in Tris-HCl buffer (50 mM, pH 8), and absorbances were measured using a quartz cuvette with 1 cm path length.

Fluorescence lifetime imaging microscopy (FLIM) study. In the FLIM study, images were captured by a confocal laser scanning microscope (Axio Observer A1) from Zeiss, coupled with a DCS-120 system from Becker & Hickl (BH) GmbH. Here, a long pass filter (HQ495LP) was utilised to block the excitation light and a picosecond diode laser (BDL-488-SMC, BH) with λ_{ex} = 405 nm was employed to excite all of the samples. For monitoring the emission, a thin band-pass filter of 525-550 nm (HQ525/50) was used, and a BH GVD-120

scan controller was used to control the scanning. The hybrid detector (BH HPM-100-40) module in the DCS-120 system was regulated by DCC-100 software. In our study, we have used 4-(dicyanomethylene)-2-methyl-6-(4-dimethylaminostyryl)-4*H*-pyran (DCM) dye as a fluorescent indicator, and a 1 mM stock solution was prepared in methanol. Next, 1 mg/mL concentration of samples (5 μL) was added with 1 mM concentration of DCM dye solution (10 μL) and incubated for a period of 15 min. Now, images were taken using a microscope and SPCImage software after putting one drop of the sample on a clean glass slide and covered with a coverslip.

Temperature dependent fluorescence study. In this study, a titration was carried out by consecutive addition of different polymers into a 2 mL of 2 μM insulin and insulin fibril solution at varied temperatures; 303 K, 308 K, and 313 K. The quenching spectra were obtained by using an exciation wavelength of 276 nm and the fluorescence emission was measured in the range 300-450 nm. Finally, all the data were analysed by using the Stern-Volmer equation (1).[10]

$$\frac{F_0}{F} = 1 + K_q t_0[Q] = 1 + K_{sv}[Q] \qquad (1)$$

Here, F_0 = fluorescence intensity of insulin protein without polymer; F = fluorescence intensity of insulin protein in the presence of polymer; K_q = quenching rate constant; t_0 = average lifespan of protein in the absence of polymer; $[Q]$ = concentration of the polymer; and K_{sv} = Stern-Volmer constant. The double-logarithm equation, shown below in equation (2) was applied to evaluate the interaction binding constant (K_b).

$$Log\frac{\Delta F}{F} = n\,Log[Q] + Log\,K_b \qquad (2)$$

where $\Delta F = F_0 - F$; n is the number of binding sites and K_b is the equilibrium binding constant. The slope and intercept of the plot of Log($\Delta F/F$) *vs* Log[Q] were used to determine the values

of K_b and n. The thermodynamic parameters were estimated from the binding constant's temperature-dependent nature by using the van't Hoff equation.[11]

Transmission electron microscopy (TEM) analysis. To observe the morphology of polymeric aggregates in an aqueous solution of pH 2, as well as to verify the changes in morphology and growing ability of fibril in the presence of different polymeric aggregates, TEM analysis was performed. 5 μM of insulin fibril sample or 0.5 mg/mL polymeric solution was added onto glow discharged carbon coated 300 mesh Cu grid, and dried under vacuum desiccator. Then, the images were taken using a JEOL JEM-2100F electron microscope.

Dynamic light scattering (DLS) and zeta potential measurements. For the determination of the average sizes of the polymeric aggregates and insulin fibrils, polymeric samples (1 mg/mL concentration in pH 2 aqueous solution) and insulin fibril (2 μM concentration) solutions were taken in 1 cm pathlength of quartz cuvette and average sizes were measured using a Malvern Nano ZS instrument. To measure the surface charge of polymers, zeta potential measurements were performed. In these measurements, the samples were prepared at pH 2, and the surface charge was determined in the same Malvern instrument.

Circular dichroism (CD) analysis. Freshly prepared insulin fibril solution alone and in the presence of glycopolymers were diluted with water, and the secondary conformation was analysed by far-UV CD spectroscopy in the region 190-240 nm using a quartz cell (0.1 cm path length) at 25 °C. The CD spectra were recorded on a Jasco J-815 CD spectrometer with a response time of 4 sec and scan rate of 50 nm/min. The secondary structural content was determined by using an online server, DICHROWEB.

Isothermal titration calorimetry (ITC) study. To investigate the interactive behaviours of native insulin or fibrils with the glycopolymeric aggregates, ITC measurements were performed. The Hamilton syringe used for ITC was filled with glycopolymer solution and

titrated into the sample cell containing native insulin or insulin fibrils in this experiment. An overall 19 successive injections was designed for each set of experiments, and injected 2 μL of polymer solution (1 mM) into the sample cell containing native insulin or insulin fibril. The time duration between two successive injections was 10 sec with a 4 min of interval between every injection. After the experiment, the heat of interaction as well as thermodynamic parameters was determined by using Microcal PEAQ-ITC software.

Hemolysis study. To find the effectivity of glycopolymers on insulin fibril (IF)-induced cytotoxicity and membrane disrupting ability of red blood cells (RBCs), a hemolysis study was performed.[12] Typically, goat blood was collected from the local market and centrifugation of the blood was carried out at 3500 rpm for a period of 15 min to isolate RBCs from buffy coat and plasma by continuously washing (× 5) with phosphate-buffered saline (pH 7.4). Next, the various incubated IFs were mixed with 1% hematocrit and incubation was continued for 40 min at 37 °C. Then, the mixture was centrifuged once again for 15 min at 3500 rpm, and the supernatant's absorbance value was measured at a fixed wavelength of 540 nm, considered as the maximum absorbance of hemoglobin.[13] The rate of hemolysis relative to Triton X-100 hemolysis were calculated for the polymers, IF, and polymer-treated IF. Hemolysis of 1% Triton X-100 with RBCs was deemed to be 100%.

Molecular dynamics (MD) simulations. The 2D structure of P(Leu-HEMA)$_5$-*b*-P(Ac-G-EMA)$_5$, P(Boc-Leu-HEMA)$_5$-*b*-P(HO-G-EMA)$_5$, and P(Leu-HEMA)$_5$-*b*-P(HO-G-EMA)$_5$ polymers was created using ChemDraw 21.0 where we have taken five repeating units in both the block, and exported to Chem3D for energy minimization. Note that 5 repeating units in both the block within the molecular structure are oligomers, and the studied interactions are based on smaller model molecules. The solution structure of insulin (PDB ID: 6QQ7)[14] was considered as the initial structure for polymer interaction analysis. Then, the 3D structures were subjected to molecular docking using autodock vina.[15] The best-ranked docked conformations

of insulin and polymers were subjected to 1 μs of all-atom MD simulations with the help of the GROMACS (version 2018.3) software package employing the GROMOS96 54A7 force field.[16,17] For the MD simulations set up for the protein-polymer complexes, the topology parameters of insulin and polymers were created employing GROMACS and PRODRG2 servers, respectively.[18] Then, the prepared protein-polymer complexes were allowed to be solvated in a dodecahedron box having a 1.0 nm distance between the edge of the box and the complex. The solvated system was then allowed to neutralize by addition of sodium or chloride ions in the simulation box. To confirm the steric clashes/geometry of the complex, the system was energy minimized using the LINCS constraints and steepest descent algorithms. After the initial minimization was completed, the whole system was equilibrated for 1 ns at 300 K degrees and 1 bar pressure using canonical (*NVT*) and isothermal-isobaric (*NPT*) ensembles. Final MD simulations of protein-polymer complexes were performed at 300 K, 1 atm pressure, and 2 fs time step for 1 μs. Using the usual GROMACS algorithms, the final MD trajectories were evaluated to get the RMSD (root mean square deviation) and RMSF (root mean square fluctuation) values. The visual analysis of the MD snapshots at 1 μs timestep is done using the PLIP server.[19] On the DIRAC supercomputer at IISER Kolkata, all of the MD simulations and outcome analysis were completed. The binding free energy was calculated for complexes using g_mmpbsa by retrieving 1000 structures from the last 100 ns MD simulation.[20]

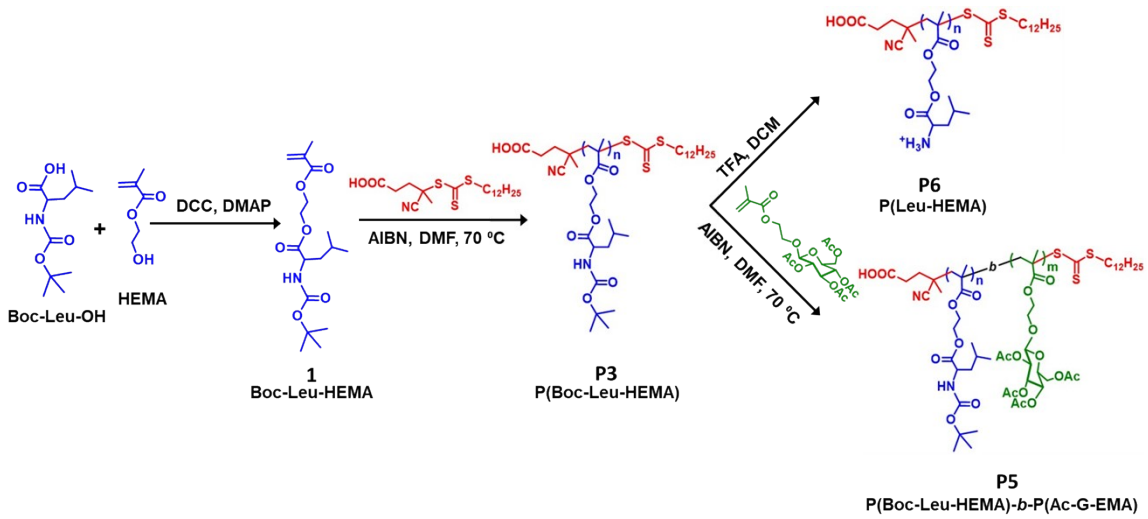

Scheme S1. Synthesis of leucine-based monomer and corresponding homopolymer by RAFT polymerization with subsequent Boc deprotection, and glycosylated block copolymer synthesis by RAFT polymerization using P(Boc-Leu-HEMA) macroCTA.

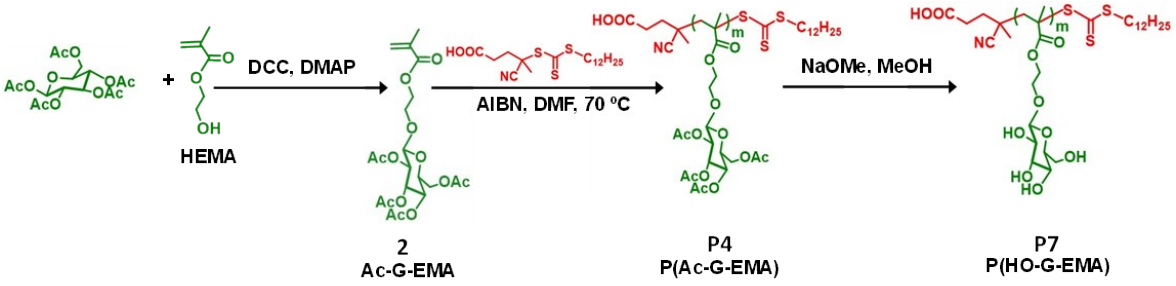

Scheme S2. Synthesis of glucose-based monomer, and corresponding homopolymer by RAFT polymerization with subsequent acetyl deprotection.

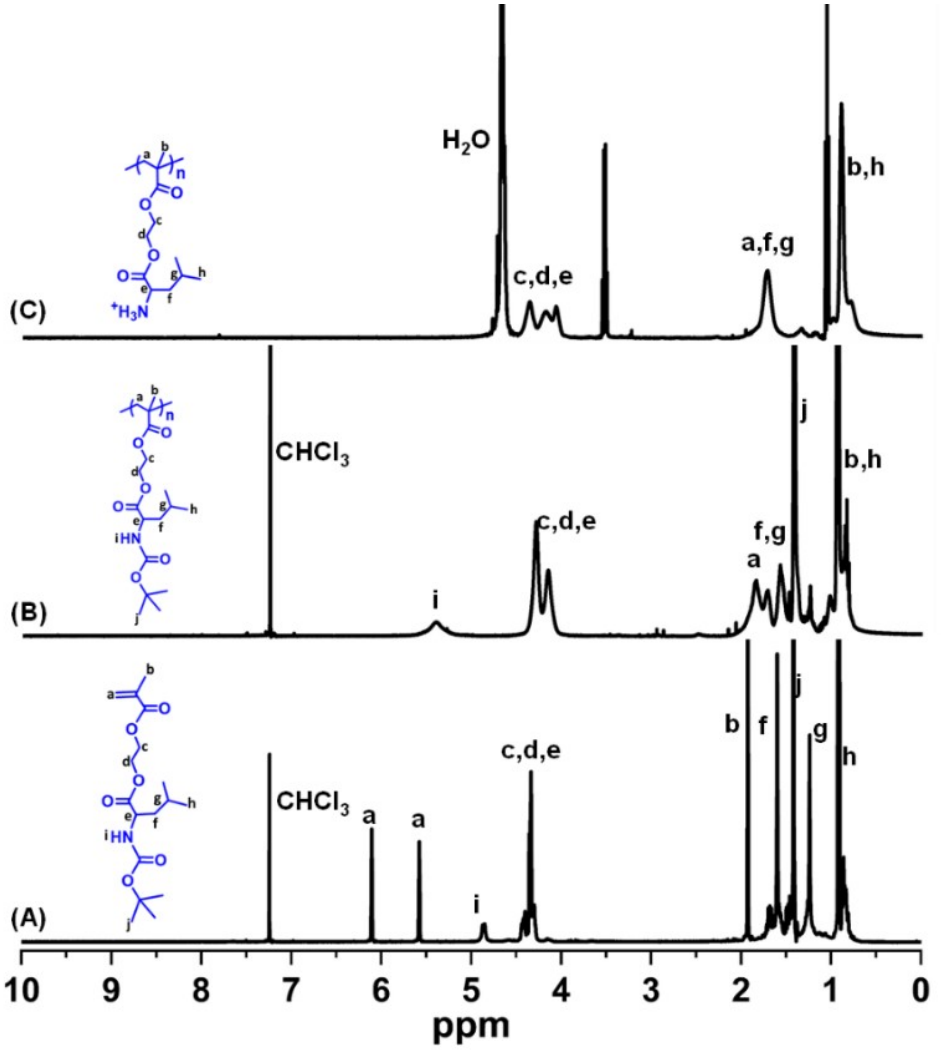

Fig. S1 ^{1}H NMR spectra of leucine-based monomer **1** (A), homopolymer **P3** (B), and respective Boc- deprotected homopolymer **P6** (C).

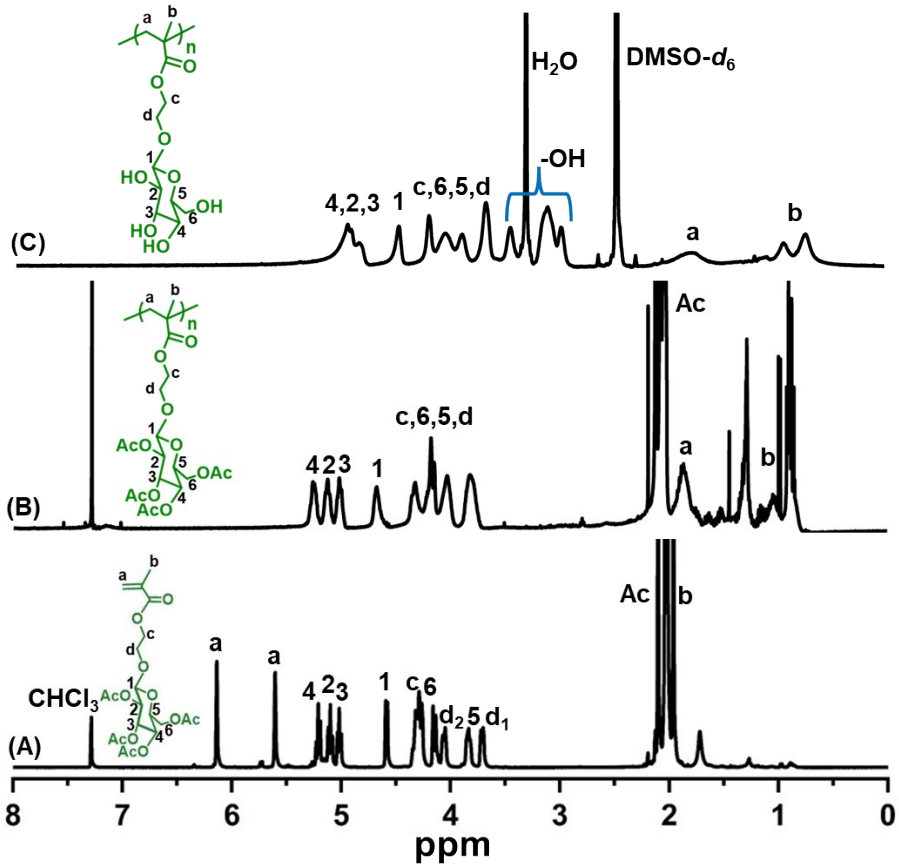

Fig. S2 ^{1}H NMR spectra of glucose-based monomer **2** (A), homopolymer **P4** (B), and corresponding acetyl deprotected homopolymer **P7** (C).

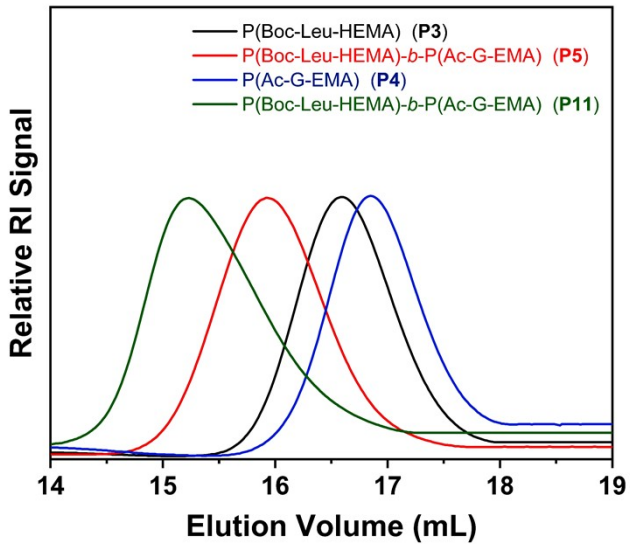

Fig. S3 Size exclusion chromatography (SEC) refractive index (RI) traces of homopolymers **P3** and **P4**, and block copolymers **P5** and **P11**.

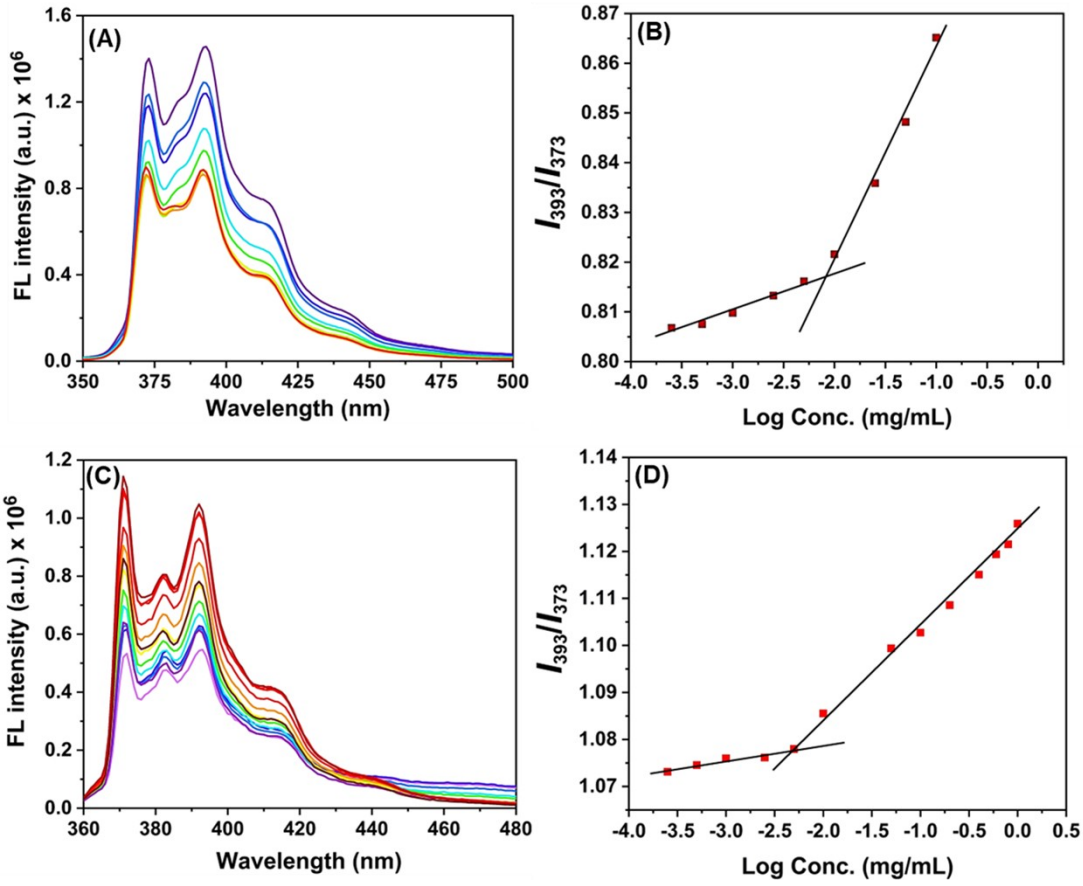

Fig. S4 Fluorescence spectra of pyrene dye at different concentrations of copolymer **P8** (image A) and **P9** (image C) in water, and plot of intensity ratio I_{393}/I_{373} *versus* logarithm of concentrations of **P8** (image B) and **P9** (image D).

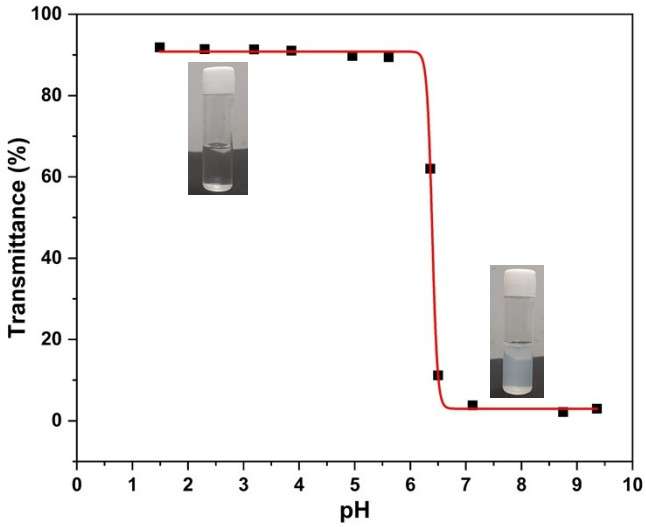

Fig. S5 Impact of pH on the polymer **P6** aqueous solution's transmittance at 500 nm.

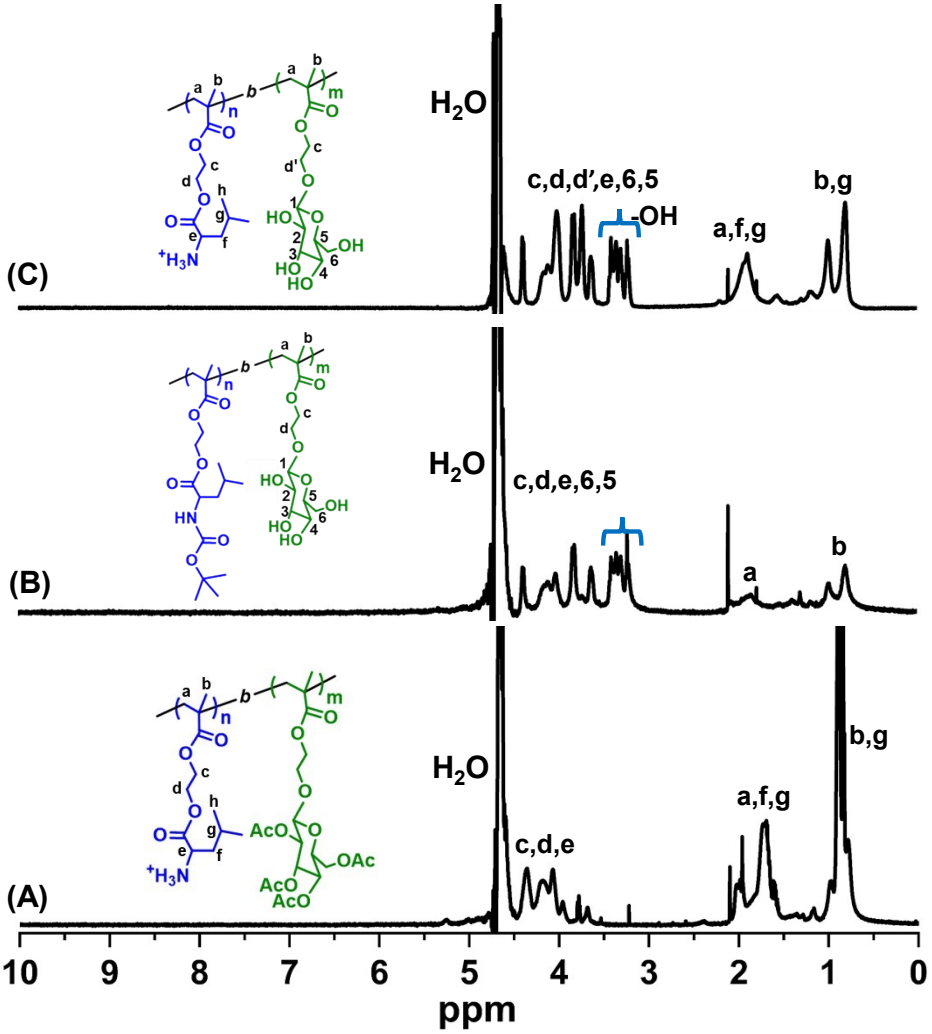

Fig. S6 (A) ^{1}H NMR spectra of polymer **P8**, (B) polymer **P9** and (C) polymer **P10** in D_2O solvent.

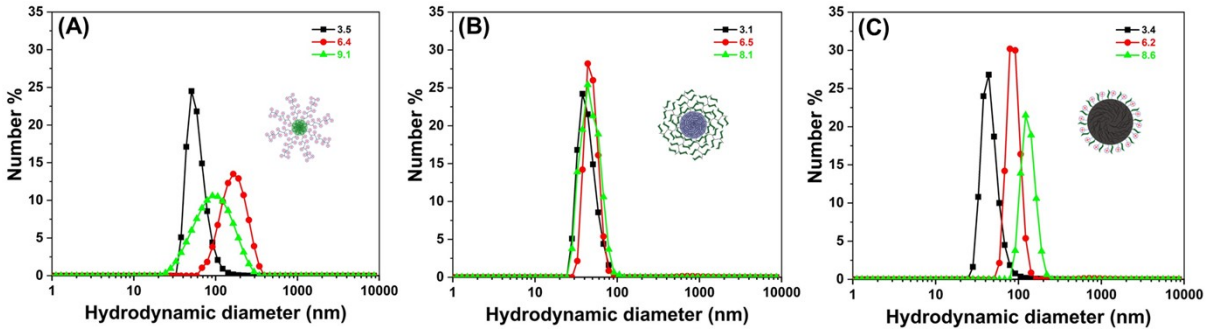

Fig. S7 Effect of pH on the size distribution of an aqueous solutions of **P8** (A), **P9** (B) and **P10** (C).

Table S1. Zeta potential results of different glycopolymers at pH 2.

Polymer	Zeta potential (mV)
P6	+13.2
P7	+2.3
P8	+11.9
P9	+5.3
P10	+10.2

Table S2. The inhibition rate of various glycopolymers on the insulin aggregation process, determined from ThT fluorescence measurements.

Sample type	Inhibitory rate (%)
Insulin fibrils + **P6**	14
Insulin fibrils + **P7**	22
Insulin fibrils + **P8**	35
Insulin fibrils + **P9**	58
Insulin fibrils + **P10**	76

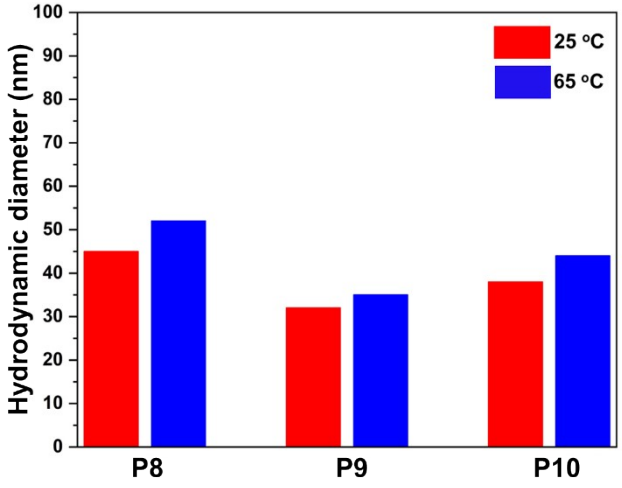

Fig. S8 Histogram of the size of different polymeric nanoassemblies at different temperatures.

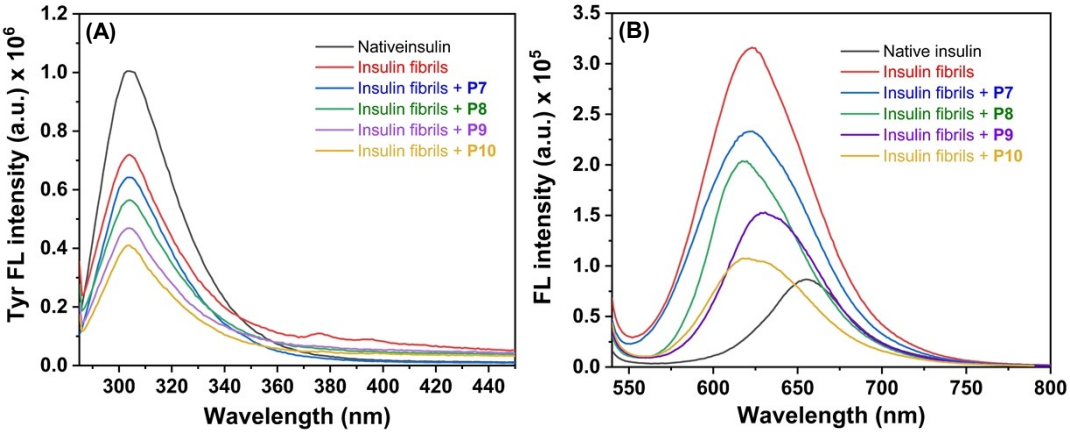

Fig. S9 (A) Tyrosine fluorescence spectra and (B) Nile red (NR) fluorescence spectra of insulin fibrils incubated alone and in the presence of different glycopolymers. Excitation wavelength (λ_{ex}) was fixed at 276 nm for Tyr fluorescence and 530 nm for NR fluorescence. Sample concentration was maintained at 5 μM for Tyr fluorescence. For NR fluorescence, the sample concentration was fixed at 2.5 μM and dye concentration was kept at 10 μM.

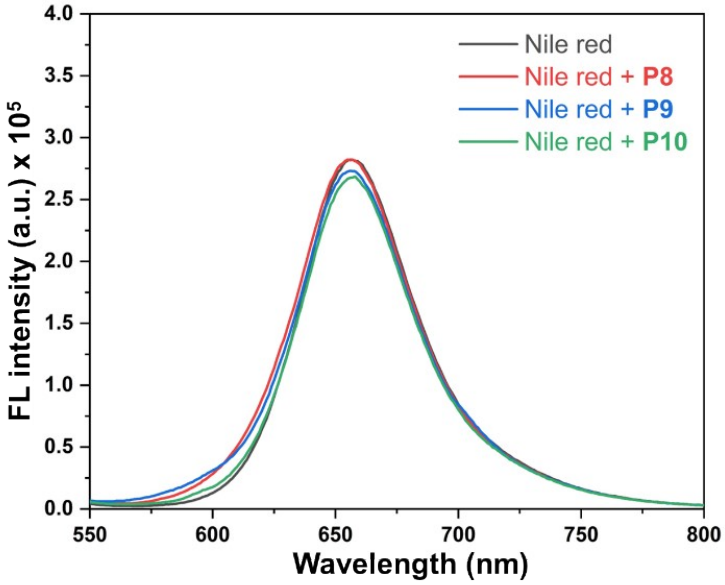

Fig. S10 Binding interaction of nile red with different polymers after 20 min of incubation.

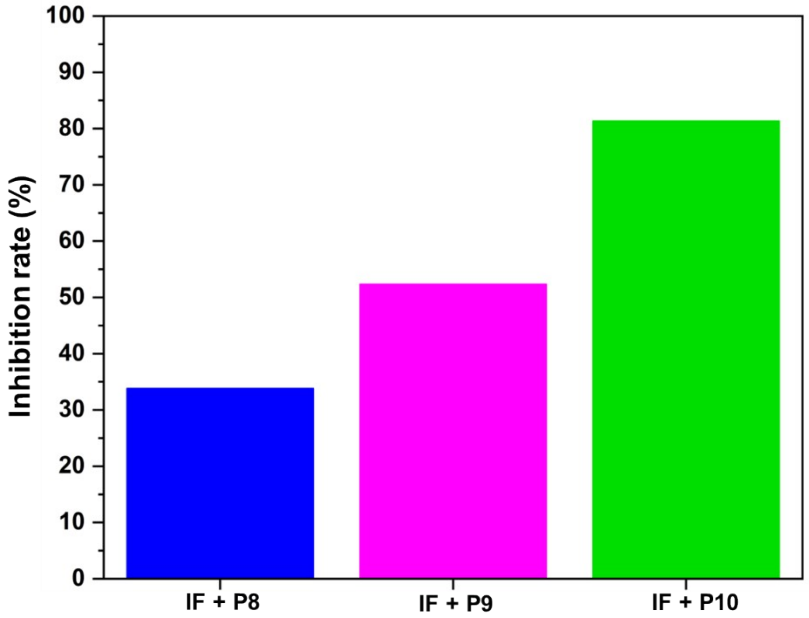

Fig. S11 Histogram of the inhibitory rate of different polymers on the insulin fibrils disintegration.

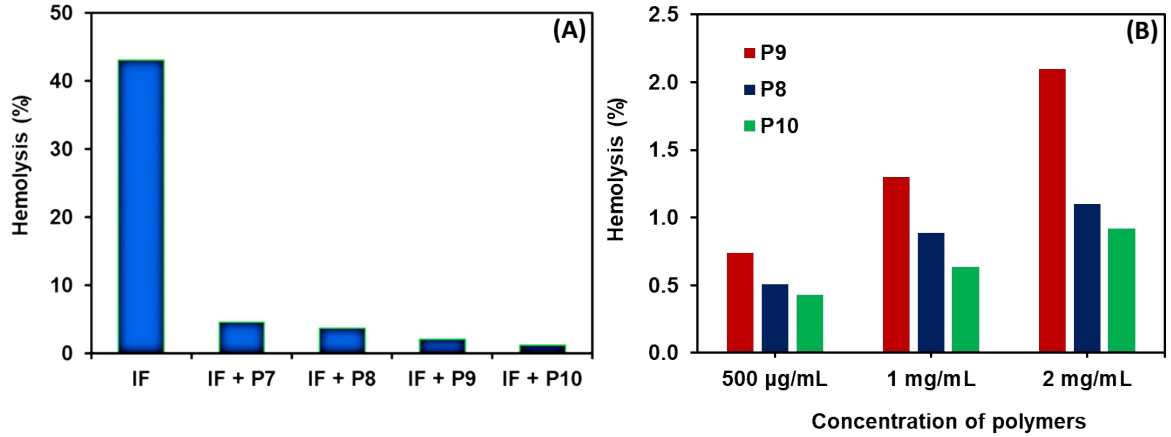

Fig. S12 (A) Histogram plot of percentage of hemolysis of IF alone and in the presence of different glycopolymeric aggregates. (B) Histogram plot of hemolytic rate of different concentrations of glycopolymers alone.

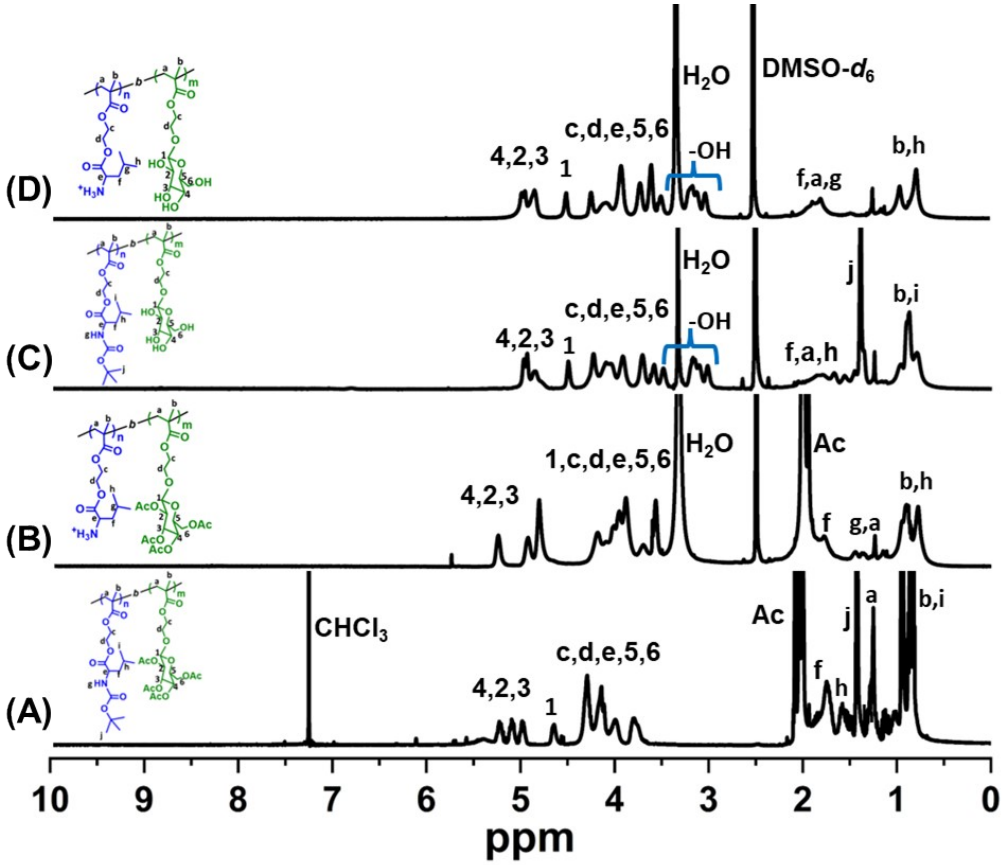

Fig. S13 ^{1}H NMR spectra of (A) **P11** in $CDCl_3$, (B) **P12**, (C) **P13** and (D) **P14** in DMSO-d_6.

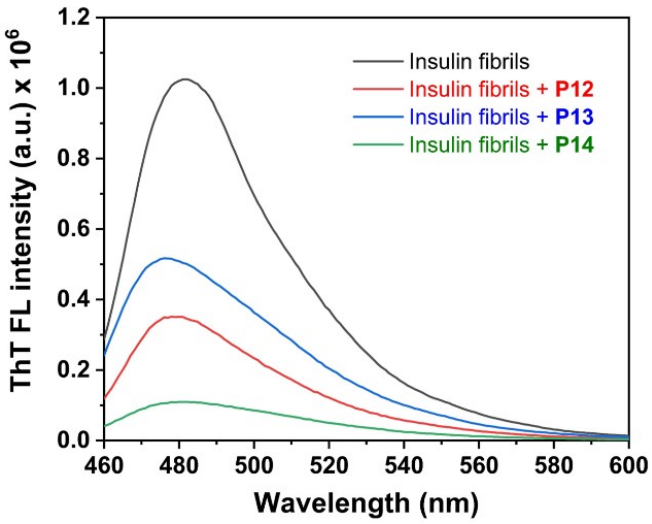

Fig. S14 ThT fluorescence emission spectra of insulin fibrils alone, and in the presence of glycopolymer **P12**, **P13** and **P14**.

Table S3. The inhibitory rate of **P12**, **P13,** and **P14** polymer treated fibril, determined from ThT fluorescence measurements.

Sample type	Inhibitory rate (%)
Insulin fibrils + **P12**	50
Insulin fibrils + **P13**	65
Insulin fibrils + **P14**	89

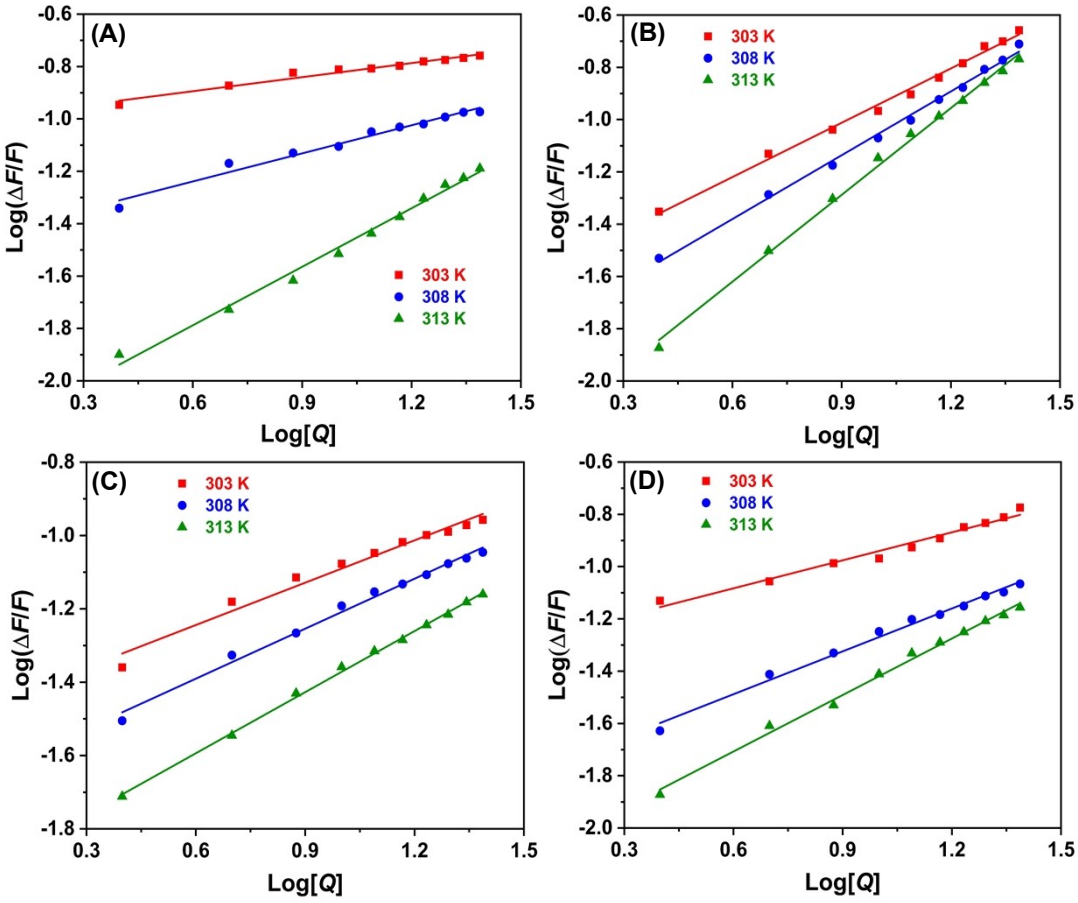

Fig. S15 Representative double logarithm plots for the interaction of (A) **P14** with native insulin; (B) **P14** with insulin oligomers; (C) **P13** with native insulin; and (D) **P13** with insulin oligomeric species at 303 K, 308 K and 313 K.

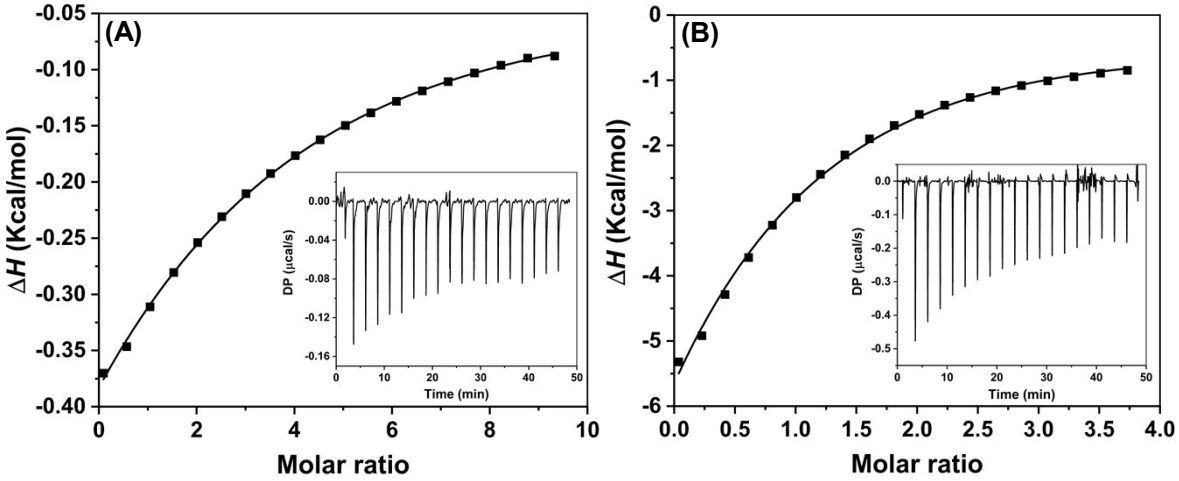

Fig. S16 ITC profiles of (A) insulin fibrils with **P12** and (B) native insulin with **P12**.

Table S4. Thermodynamic parameters for the interactions of insulin monomer/oligomers with **P13** and **P14** polymeric nanoassemblies.

System	Temperature (K)	ΔG^0 (KJ/mol)	ΔH^0 (KJ/mol)	ΔS^0 (J/mol K)
P13-Native insulin	303	-45.4	-66.7	-70.3
	308	-45.0		
	313	-44.7		
P13-Insulin oligomers	303	-126.9	-186.2	-195.5
	308	-125.9		
	313	-125.0		
P14-Native insulin	303	-136.1	-202.8	-220.0
	308	-135.0		
	313	-134.0		
P14-Insulin oligomers	303	-252.7	-375.5	-405.2
	308	-250.6		
	313	-248.7		

Table S5. Interaction map of insulin protein and different glycopolymers from 1 μs MD snapshots.

Complex A

Hydrogen Bonds			
Residue	AA	Donor Atom	Acceptor Atom
1A	GLY	1 [N3]	993 [O3]
3B	ASN	352 [Nam]	1011 [O3]
3B	ASN	779 [N3]	351 [O2]
4A	GLU	984 [O3]	56 [O-]
8A	ALA	781 [N3]	105 [O2]
9A	SER	113 [O3]	1018 [O3]
15A	GLN	206 [Nam]	963 [O3]
18A	ASN	245 [Nam]	954 [O3]
30B	ALA	766 [Nam]	998 [O3]
30B	ALA	998 [O3]	775 [O co2]
3B	ASN	1[N3]	20[02]

Hydrophobic Interactions			
Residue	AA	Ligand Atom	Protein Atom
4A	GLU	863	48
8A	ALA	925	100
29B	LYS	857	754
30B	ALA	876	770

Electrostatic Interactions		
Residue	AA	Ligand Group
29B	LYS	COO^-
29B	LYS	COO^-

Complex B

Hydrogen Bonds			
Residue	AA	Donor Atom	Acceptor Atom
1A	GLY	224 [N3+]	92 [O2]
3A	VAL	175 [O3]	239 [O2]
5A	GLN	259 [Nam]	60 [O2]
5B	HIS	135 [O3]	429 [Nar]
8B	GLY	177 [O3]	447 [O2]
12A	SER	302 [O3]	15 [O2]
14A	TYR	8 [Nam]	314 [O2]
15A	GLN	330 [Nam]	60 [O2]
18A	ASN	355 [Nam]	36 [O2]
26B	TYR	595 [O3]	177 [O3]
29B	LYS	216 [O3]	613 [O2]
30B	ALA	214 [O3]	622 [O2]

Hydrophobic Interactions			
Residue	AA	Ligand Atom	Protein Atom
4A	GLU	100	247
5A	GLN	52	256
10A	VAL	64	290
17A	GLU	4	344
19A	TYR	38	366
29B	LYS	89	615

Electrostatic Interactions		
Residue	AA	Ligand Group
29B	LYS	COO^-
29B	LYS	COO^-

Complex C

Hydrogen Bonds			
Residue	AA	Donor Atom	Acceptor Atom
1A	GLY	1 [N3+]	578 [O3]
5A	GLN	36 [Nam]	476 [O2]
8A	ALA	50 [Nam]	540 [O3]
9A	SER	484 [N3]	60 [O3]
10A	VAL	61 [Nam]	528 [O3]
12A	SER	433 [N3]	79 [O3]
12A	SER	79 [O3]	416 [O2]
15A	GLN	107 [N3]	476 [O2]
29B	LYS	387 [Nam]	578 [O3]
30B	ALA	548 [O3]	401 [O2]

Hydrophobic Interactions			
Residue	AA	Ligand Atom	Protein Atom
5A	GLN	491	34
14A	TYR	405	96
15A	GLN	421	105

Table S6. MM/PBSA based binding energy calculation.

Various energy (kJ/mol)	Complex A	Complex B	Complex C
van der Waal energy	-266.1 +/- 39.3	-317.9 +/- 37.7	-252.1 +/- 48.2
Electrostatic energy	-381.8 +/- 121.3	-54.1 +/- 60.2	-377.4 +/- 71.9
Polar solvation	229.4 +/- 84.8	272.2 +/- 92.4	267.6 +/- 71.9
SASA energy	-28.1 +/- 5.0	-35.4 +/- 4.4	-28.3 +/- 4.1
Binding energy	-446.7 +/- 85.1	-135.3 +/- 61.5	-390.3 +/- 76.5

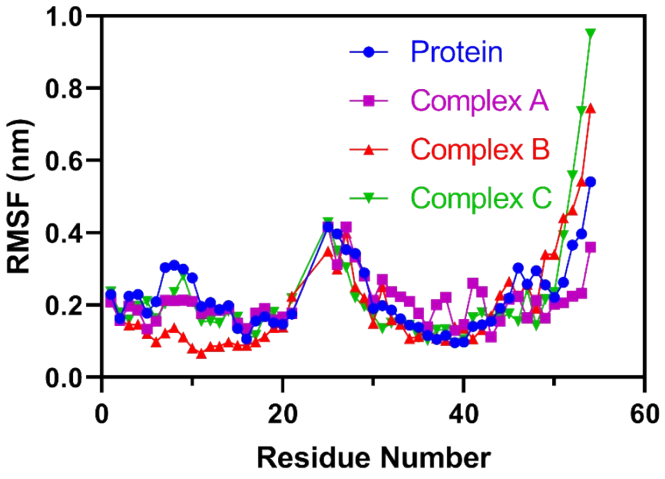

Fig. S17 Molecular dynamics trajectory plots for root mean square fluctuation (RMSF) of backbone atoms present in protein, interacting with different polymers derived from 1 μs MD simulations.

REFERENCES

1. S. Kumar, R. Acharya, U. Chatterji and P. De, *J. Mater. Chem. B*, 2013, **1**, 946-957.

2. K. Bauri, S. Pant, S. G. Roy and P. De, *Polym. Chem.*, 2013, **4**, 4052-4060.

3. S. Kumar, B. Maiti and P. De, *Langmuir*, 2015, **31**, 9422-9431.

4. B. Lu, Y. Li, Z. Wang, B. Wang, X. Pan, W. Zhao, X. Ma and J. Zhang, *New J. Chem.*, 2019, **43**, 12275-12282.

5. P. Hanczyc, P. Słota, C. Radzewicz and P. Fita. *J. Photochem. Photobiol. B: Biol.*, 2022, **228**, 112392(1-7).

6. S. A. Hudson, H. Ecroyd, T. W. Kee and J. A. Carver, *FEBS J.*, 2009, **276**, 5960-5972.

7. S. Ghosh, N. K. Pandey and S. Dasgupta, *Int. J. Biol. Macromol.*, 2013, **54**, 90-98.

8. B. Katebi, M. Mahdavimehr, A. A. Meratan, A. Ghasemi and M. Nemat-Gorgani, *Arch. Biochem. Biophys.*, 2018, **659**, 22-32.

9. Y. M. Kwon, M. Baudys, K. Knutson and S. W. Kim, *Pharm. Res.*, 2001, **18**, 1754-1759.

10. J. R. Lakowicz, *Principles of Fluorescence Spectroscopy*; Springer US: Boston, MA, 2006; pp 27–61.

11. Y. J. Hu, Y. Liu, J. B. Wang, X. H. Xiao and S. S. Qu, *J. Pharm. Biomed. Anal*., 2004, **36**, 915–919.

12. K. H. Yu and C. I. Lee, *Pharmaceutics*, 2020, **12**, 1081-1090.

13. P. Ghosh, J. Patwari and S. Dasgupta, *J. Phys. Chem. B*, 2017, **121**, 1758-1770.

14. K. Kurpiewska, A. Miłaczewska and K. Lewiński, *J. Mol. Struct.*, 2020, **1202**, 127251(1-8).

15. O. Trott and A. J. Olson, *J. Comput. Chem.*, 2010, **31**, 455-461.

16. D. Van Der Spoel, E. Lindahl, B. Hess, G. Groenhof, A. E. Mark and H. J. C. Berendsen, *J. Comput. Chem.*, 2005, **26**, 1701-1718.

17. N. Schmid, A. P. Eichenberger, A. Choutko, S. Riniker, M. Winger, A. E. Mark and W. F. van Gunsteren, *Eur. Biophys. J.*, 2011, **40**, 843-856.

18. A. W. Schüttelkopf and D. M. F. van Aalten, *Acta Crystallogr. D Biol. Crystallogr.*, 2004, **60**, 1355-1363.

19. M. F. Adasme, K. L. Linnemann, S. N. Bolz, F. Kaiser, S. Salentin, V. J. Haupt and M. Schroeder, *Nucleic Acids Res.*, 2021, **49**, W530-W534.

20. R. Kumari, R. Kumar and A. Lynn, *J. Chem. Inf. Model.*, 2014, **54**, 1951-1962.